OXIDATION OF UO2 AND FISSION PRODUCT RELEASE AT 400-1000°C IN AIR

D.R. McCRACKEN

Atomic Energy of Canada Limited, Research Company Chalk River Nuclear Laboratories Chalk River, Ontario, KOJ 1J0

ABSTRACT

Studies of the oxidation of unirradiated UO2 pellets in air show two distinct types of oxidation with a change in mechanism at 600-700°C. At temperatures ≤600°C, U₃0₈ spalls as small particles, 1-15 um, as soon as it forms. At 700°C the $\mathrm{U}_3\mathrm{O}_8$ starts to form a cohesive structure in which grain growth occurs in the direction of the oxygen gradient. At higher temperatures ≥800°C the U308 propagates by rapid grain growth, which sweeps through the grains of irradiated UO2, producing large crystals of U₃0₈, ≥1 mm. succinctly, at T ≤ 600°C fragmentation accompanies the formation of $\rm U_3O_8$ while at T \geq 800°C, rapid grain growth occurs. It was observed that in the first temperature region, volatile fission product releases are small, while in the second region, 100% release can be correlated with $\rm U_3O_8$ formation. This is supported by data in the literature. In the first region, only the grain boundary inventory is released while in the other, 100% of the Xe, Kr, Ru, Sb, Cs and I are released. The Ru, probably as RuO2, reacts rapidly with Zr so that little can escape from an element or pressure tube; iodine probably as I2, plates out rapidly on steel so that little of this can escape from a real system. Te releases are small, as it plates out rapidly on both Zr and steel.

It appears that, within the error of measurements, burnup does not greatly affect rates of fission product release and oxidation in air at 400-1000°C, so that oxidation rate data gathered using unirradiated pellets can be applied to irradiated fuel.

INTRODUCTION

Irradiated uranium dioxide fuel can conceivably be exposed to a hot oxidizing atmosphere as a result of the following accidents: end fitting failures in CANDU reactors; accidents during transportation or storage of fuel; and finally during destructive investigations, e.g. metallographic examination of thermally hot fuel.

Since fission product release can occur as a result of oxidation, data is necessary to predict when significant oxidation will begin and the subsequent extent of deterioration when fuel pellets are exposed to air or steam at high temperatures.

It had previously been determined that rates of oxidation could depend on the temperature of reaction (1-6), density of $\rm UO_2$ (1,6), method of preparation of sample (6,7), partial pressure of oxygen (6, 8-10), and the surface area of the sample (3,6,9,10), however, details of movement of oxidation fronts and mechanistic interpretation were scant.

This paper presents a review of data, current thinking and knowledge based on a large number of experiments carried out at CRNL over the past few years. Some of this work is reported in detail elsewhere (11-13).

Two parallel studies have been carried out in this work: a mechanistic study of the oxidation of unirradiated pellets in air; and a study of fission product release during oxidation in air of irradiated fuel.

In the former, well-characterized unirradiated CANDU reactor fuel pellets were used. The purpose was to investigate the dependence of UO₂ oxidation on temperature, rate of air supply and residence time; to determine the rate controlling steps and rate of oxygen penetration; and to characterize the oxidation products and size of fragments. The advantage of using large uniform samples is that the movement of oxidation fronts is readily observed.

In addition, detailed metallography was related to X-ray diffraction studies of the oxidized ${\tt UO}_2$.

In the fission product release program, low and high burnup fuels were oxidized in-cell, and on-line measurements were made of releases of volatile fission products. The apparatus was subsequently dismantled and the fission product distributions throughout the pipework were measured.

EXPERIMENTAL

Samples were heated in argon, then once at temperature they were exposed to air at a controlled flow-rate. This simulates the accidental exposure of hot UO₂ to air.

In the fundamental study of the oxidation of UO2, standard unirradiated Bruce type or G-2 fuel pellets were brought to temperature in a flowing argon stream in a quartz furnace tube and crucible. Reference 11 gives details of pellets. Once at temperature, air was introduced at a controlled flow-rate for a set time before cooling in argon.

The Debye-Scherrer powder method was used to perform X-ray diffraction analyses on powder spalled during oxidation and on powder obtained by scraping the edges and kennels of oxidized pellets. X-ray diffractometry was used for quantitative analyses. Standard reference cards were used for identification of X-ray lines (14).

Metallography was done using standard procedures and an etchant consisting of a 9:1 mixture of 30% $\rm H_2O_2$ and concentrated $\rm H_2SO_4$. Examination and photography was done using a Vickers Projection

microscope. When results from metallography needed confirmation, pieces of the sample were crushed and ground into a fine powder, and X-ray diffraction was performed.

Fission product release studies were done in hot cells. Zirconium lined muffle or tube furnaces were used to heat irradiated fuel fragments contained in quartz boats. A sweep-gas technique was used in which the fuel was exposed to argon during heat up (20°/min). The atmosphere was then changed to air once the sample was at temperature. The gas flowed over the fuel, past a gamma-ray spectrometer, then to a series of traps (Figure 1). The last trap in the system was charcoal at -70°C to trap all Xe, Kr, and any iodine which escaped the first series of traps. After an oxidation run, all pipework from the furnace tube to the cold trap was counted for deposited fission products. Generally the bulk of the piping was polyethylene tubing, which resists picking up activity, while the rest was steel.

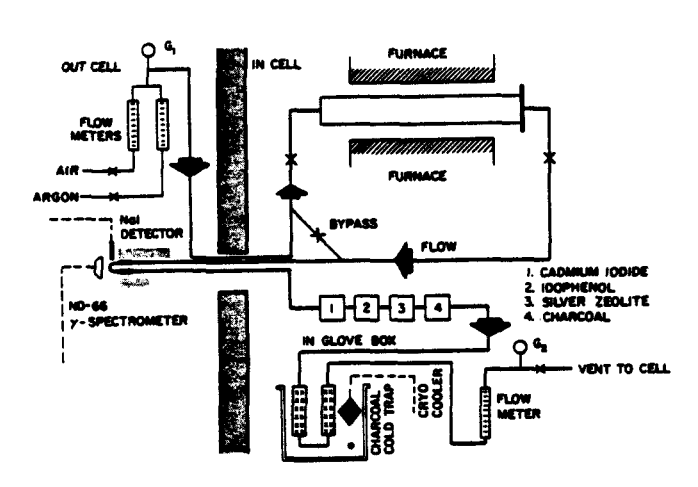


FIGURE 1: General description of apparatus.

Xenon calibration samples were injected into the argon flow-system while it was at temperature.

On the basis of previous experiments, gas flows were selected to ensure that particulate matter was not transported in the system.

MECHANISTIC STUDIES OF UO2 OXIDATION IN AIR

In test runs, samples were heated and cooled using only argon gas to confirm that negligible oxidation (0.001% weight gain) occurred, and no fragmentation occurred with heating rates of 5-100°C/min.

It was found that in a pure form, $\rm U_40_9$ has an equiaxed grain structure which is identical to that of $\rm U0_2$. The Widmanstatten needle-like structure reported previously (15,16) was observed only during the transition from $\rm U0_2$ to $\rm U_40_9$ when both oxides exist together. $\rm U_30_7$ was observed by X-ray diffractometry in samples oxidized at $\rm 400\,^\circ C$ and $\rm 500\,^\circ C$ but metallographically it does not obviously have the characteristic coaxial grain structure observed at lower temperatures (12).

Much of the $U_3 \\ ^0 8$ powder which spalled from pellets in these experiments was sub-micron in size. It was found that this fine powder was very easily disturbed: oxidation at a flow rate of 2000 mL/min in the apparatus caused entrainment and distribution problems.

Oxygen depletion of the air supply was observed only at 500 °C and 50 mL/min of airflow.

Details of ceramography and oxide structures are given in References 11-13.

Oxidation at 400°C

At this temperature, the oxidation of 00_2 to U₃0₈ is very rapid. A determination of weight gain versus time, using an airflow of 50 mL/min, revealed an induction period then a short period of fast oxidation, followed by a plateau before rapid and complete oxidation to U308 (Figure 2). To check if the induction period or plateau depended on oxygen concentration or the finite time which it takes air to displace argon, oxidation was repeated using airflows of 500 mL/min and 2000 mL/min. The results in Figure 2 clearly show a strong effect of oxygen concentration on the kinetics of the oxidation process. The plateau observed at 0.5 weight% at 50 mL/min, disappears at higher flow rates, while the overall oxidation rate increases by about a factor of three. The induction period was not affected by changing the flow rate.

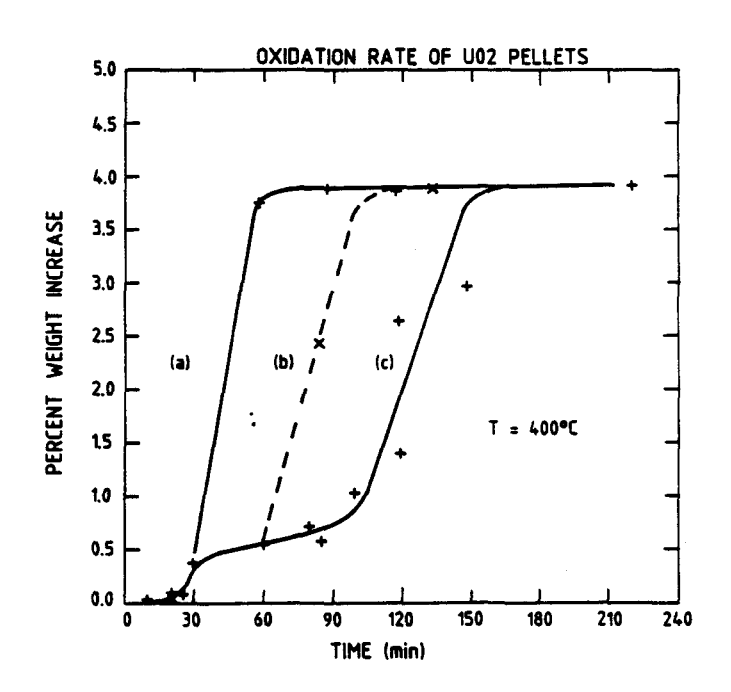


FIGURE 2: Oxidation at 400°C.

- (a) Airflow = 2000 mL/min.
- (b) Airflow = 500 mL/min; not well defined: slope set between those of (a) and (c).
 - c) Airflow = 50 mL/min; independent results of two experimenters using different flowmeters gave similarly shaped curves probably offset due to small differences in flow rate. One average curve is drawn through the data.

Photographs were taken of microstructures to determine the products and rates of movement of oxidation fronts. On the edge of all oxidized samples, a thin layer of oxide with a characteristic Widmanstatten structure of mixed oxide was observed. X-ray diffraction showed that this was a mixture of U_3O_7 and U_4O_9 in UO_2 . Above 500°C, the U_3O_7 disappeared and U409 became the main intermediate between U_{02} and U_{308} . For convenience, the mixed oxide U_{307}/U_{409} is referred to elsewhere in this section as $\rm U_4 O_9$. Very small quantities of $\rm U_3 O_8$ were loosely attached as dust to the outside of the U_4O_9 . The U_3O_8 particles were too small, 10 μ m, to show any grain structure even under polarized light. Comparable U409 thicknesses were seen for pellets oxidized for the same time but at different flow rates, even though they differed greatly in the degree of oxidation of the pellet (Figure 2), and in the size of the remaining core of UO2.

Approximate thicknesses of $\rm U_4O_9$ layers are summarized in Table 1. From 30-60 minutes at 50 mL/min there is little change in $\rm U_4O_9$ thickness.

TABLE 1: THICKNESS OF LAYERS AFTER OXIDATION AT 400°C

Airflow mL/min	Time	U409 (цт)	
			
50	10	30	
	20	25-50	
	30	75 -9 0	
	60	40-100	
	85	110	
	100	140	
	150	150	
500	85	110	
2000	30	60	

Oxidation at 500°C

The oxidation rate at 500°C was the fastest observed. Weight gain versus time curves are plotted for airflows of 50 mL/min and 500 mL/min in Figure 3. The curves are approximately linear at early times with no indication of an induction period. During oxidation at the airflow of 50 mL/min, the ratio of $N_2 \colon 0_2$ in the exit gas was $9 \colon 1$. At 500 cc/min there was no significant oxygen depletion, and the rate was faster than that observed at 50 mL/min.

Examination of the oxidized samples revealed that $\rm U_3O_8$ as a fine powder began to spall off the pellet after only 15 minutes residence time in the oxidizing atmosphere. A Widmanstatten structure of $\rm U_3O_7/\rm U_4O_9$ in $\rm UO_2$ was observed along the edge of each pellet, while the equiaxed structure of $\rm UO_2$ was observed in the interior of each pellet. Approximate thicknesses of the $\rm U_4O_9$ layer and the weights of $\rm U_3O_8$ powder are summarized in Table 2. $\rm U_3O_8$ only adhered very lightly as a fine dust, no more than $\rm 2O-4O~\mu m$ in thickness. Essentially it spalls as soon as it forms, similar to its behaviour at $\rm 4O0~^\circ C$. Some clustering of the powder was observed at longer times.

Oxidation at 600°C

Oxidation kinetics at 600°C are similar to but slower than those at 500°C: the weight change versus

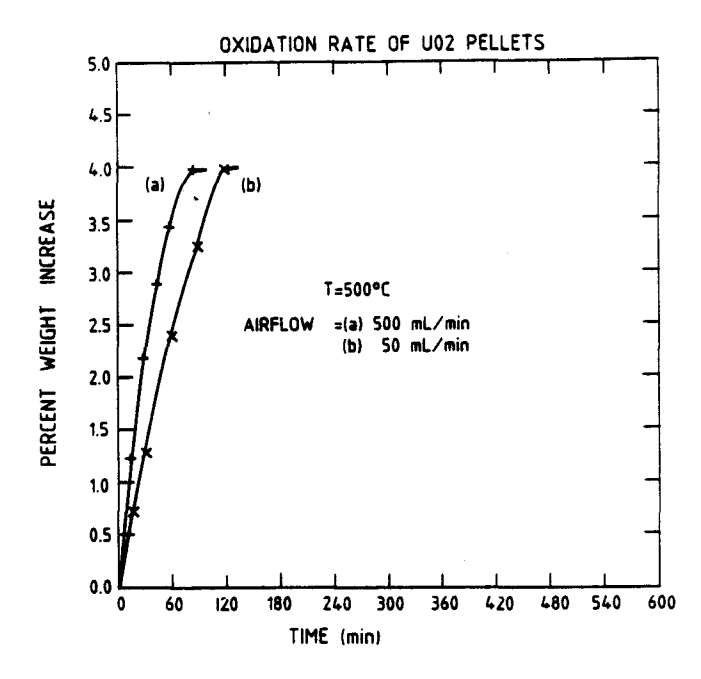


FIGURE 3: Oxidation at 500°C.

TABLE 2: OXIDATION PRODUCTS AT 500°C

	500 cc/min	50 cc/min		
Time U ₄ O ₉ (min) Thickness (µm)		^U 4 ^O 9 Thickness (um)		
15	140	140		
60	140	600		

time curve shows good linear kinetics from time zero (Figure 4); there is no induction period; the pellet steadily grows smaller with time. Instead of spalling as powder, however, much of the $\rm U_3O_8$ is in small lumps and flakes which break into powder when touched even lightly. On occasions, this powder consisted of small needles of $\rm U_3O_8$, typically 0.5 x 10 μm in size. The fragile oxidized layer on a pellet was up to 4 mm thick. Successive oxidation layers spalled off forming an accordion-like structure (11,12).

Ceramography showed structures similar to those observed at 500°C, but the $\rm U_3^{}0_8$ was in thin fragile layers.

Oxidation at 700°C

Oxidation at this temperature is significantly different to that at lower temperatures. The slower kinetics of oxidation (Figure 5), visual appearance, and ceramography of oxidized pellets are all noticeably different from those at lower temperatures.

The kinetics correspond to a protective layer which ultimately goes into breakaway corrosion. Spalled material consists of coarse particles rather than dust.

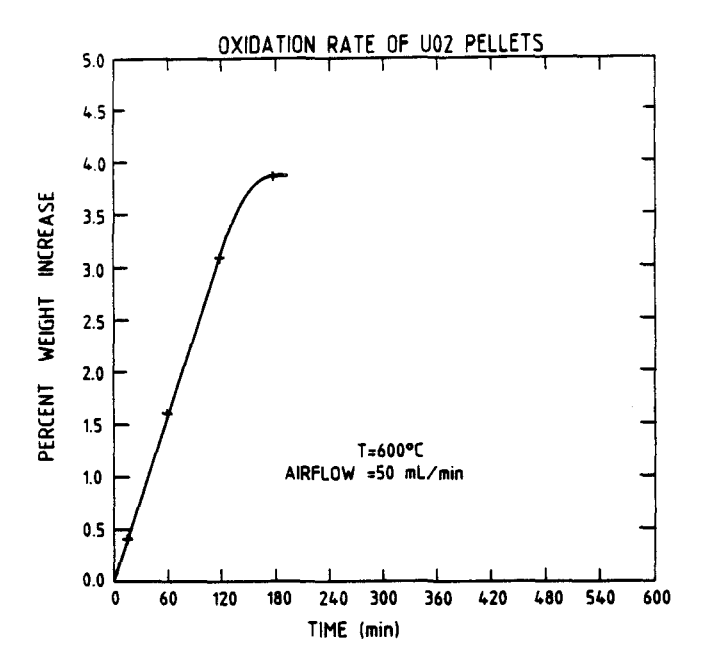


FIGURE 4: Oxidation at 600°C.

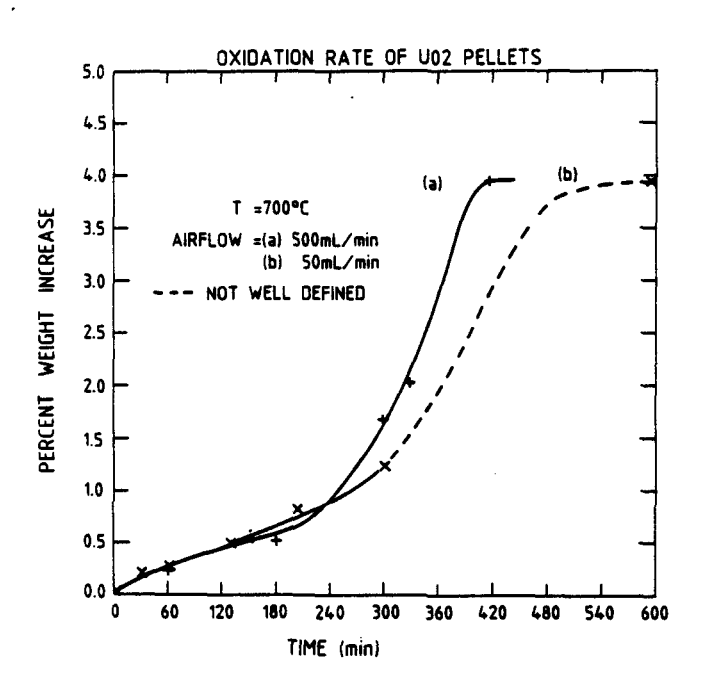


FIGURE 5: Oxidation at 700°C.

Ceramographic examination revealed a thin layer (40 $\mu m)$ of material bonded around the perimeter of the pellet. This material responded to polarized light but did not etch after one minute in the standard $\rm U0_2$ etchant. These characteristics are typical of $\rm U_30_8$. Underlying the $\rm U_30_8$ layer was the Widmanstatten structure of $\rm U_40_9$. This structure gradually changed to that of pure $\rm U0_2$ in the centre of the pellet. This continuous tight layer of $\rm U_30_8$ observed at 700°C, contrasts markedly with the loose aggregates of powdered $\rm U_30_8$ observed at lower temperatures.

Some details of the oxide layers are summarized in Table 3.

TABLE 3: OXIDATION PRODUCTS AT 700°C

Flowrate	500 cc/min		50 cc/min		
Time (min)	^U 4 ^O 9	<u>"308</u>	U409	U308	
60	0.5 mm.	40 µm	-alrega	-	
180	0.9 mm	60 µш			
300	0.9 mm	7.48 g	0.45 mm	4.7 g	

- not measured

Oxidation at 800°C

The kinetics of weight gain at 800°C (Figure 6) are very similar to those at 700°C (Figure 5), however, fragmentation of the pellet is more rapid; and there is a shorter plateau in the weight gain curve.

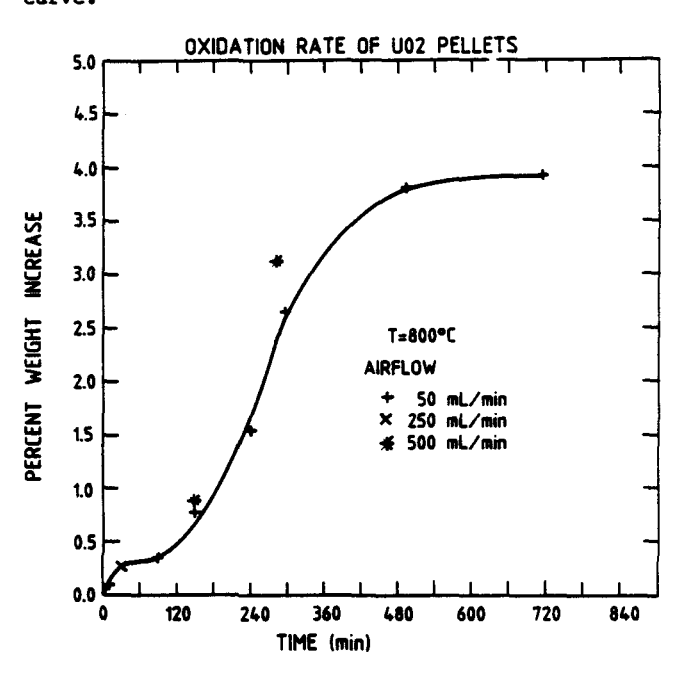


FIGURE 6: Oxidation at 800°C.

At early times, the pellet surface appeared shiny and brittle and an oxidized surface layer was clearly observed. The pellet core was brittle, had a shiny appearance when broken for examination, and was identified as $\rm U0_2/U_40_9$ by both X-ray diffraction and metallography. At longer times large pieces spalled off ultimately ending up as coarse lumps of $\rm U_30_8$, several mm in size.

Polarized light revealed a columnar grain structure of $\rm U_3O_8$ surrounding both the pellet and large spalled fragments. Another important feature was that stresses generated by the $\rm U_3O_8$ had circumferentially cracked the pellet core. This did not occur at lower temperatures.

Oxidation at 900°C

The weight change curve is closer to linear at $900\,^{\circ}\text{C}$ than at $800\,^{\circ}\text{C}$, and the overall rate is slower (Figure 7). This is compatible with the visual and metallographic observations.

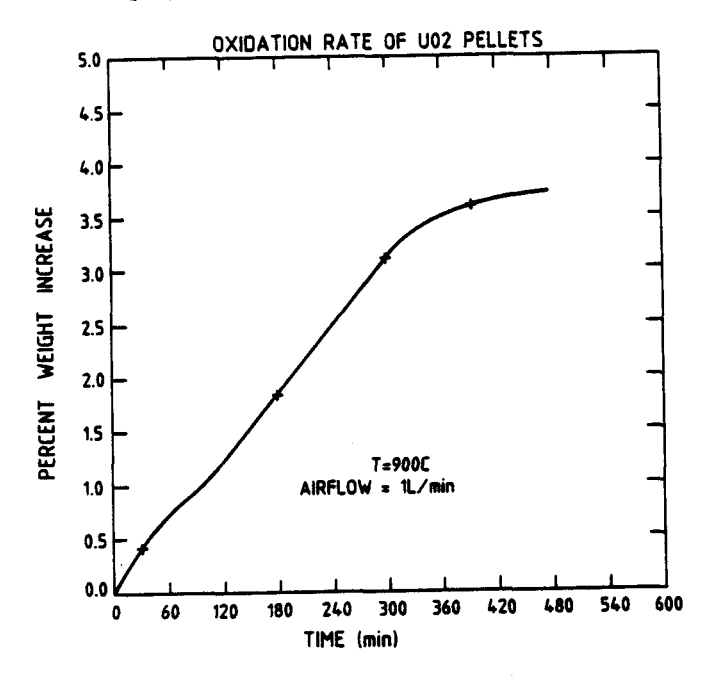


FIGURE 7: Oxidation at 900°C.

After 30 minutes a compact and complete layer of $\rm U_3O_8$ had bonded strongly to the pellet core. At longer times, the expansion of this tightly bound $\rm U_3O_8$ generated sufficient stresses to cause RADIAL cracking of the pellet core, and consequent fragmentation of the pellet into large pieces (Figure 8). X-ray diffraction confirmed the large fragments to be mixtures of $\rm U_3O_8$, $\rm U_4O_9$ and $\rm UO_2$, while small fragments were $1002~\rm U_3O_8$. The final completely oxidized sample consisted of $\rm U_3O_8$ in a whole range of sizes from 1 mm up to 4 mm, most of it being on the large side.

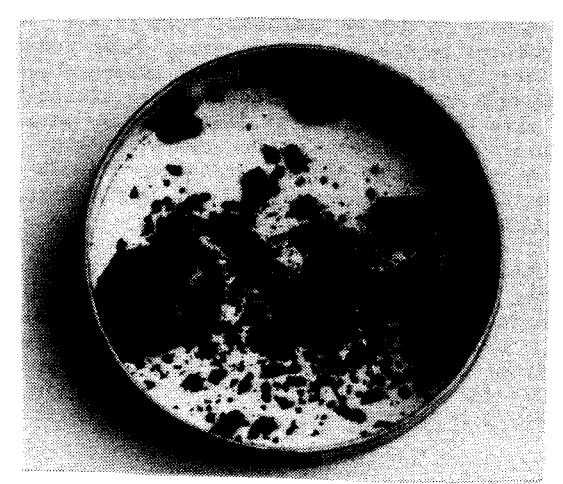


FIGURE 8: Example of a pellet oxidized at 900°C for 180 minutes at an airflow of 1 L/min. The U₃0₈ layer is clearly observable, also the RADIAL CRACKING which it has induced in the pellet core.

Examination of samples under polarized light showed that the $\rm U_3O_8$ grows in long needles from the surface and in the direction of the oxygen concentration gradient. A Widmanstatten grain structure readily attributable to $\rm U_4O_9$ in $\rm UO_2$ was observed in oxidized fragments after partial oxidation. X-ray diffraction confirmed the presence of $\rm U_4O_9$. A layer of dark grains, underlying the $\rm U_3O_8$, is also attributed to $\rm U_4O_9$, or some higher oxide with a similar X-ray diffraction pattern.

Oxidation at 1000°C

Oxidation rates at this temperature were much the slowest of those investigated. Oxidation was not complete after 10 hours. The weight gain versus time curves for airflows of 50 mL/min and 500 mL/min are shown in Figure 9. They begin with a rapid reaction, independent of oxygen supply within experimental error. The rate then decreases with time, becoming constant after 180 minutes. The final slope is slightly greater with the higher airflow. No oxygen depletion was observed at either flow rate.

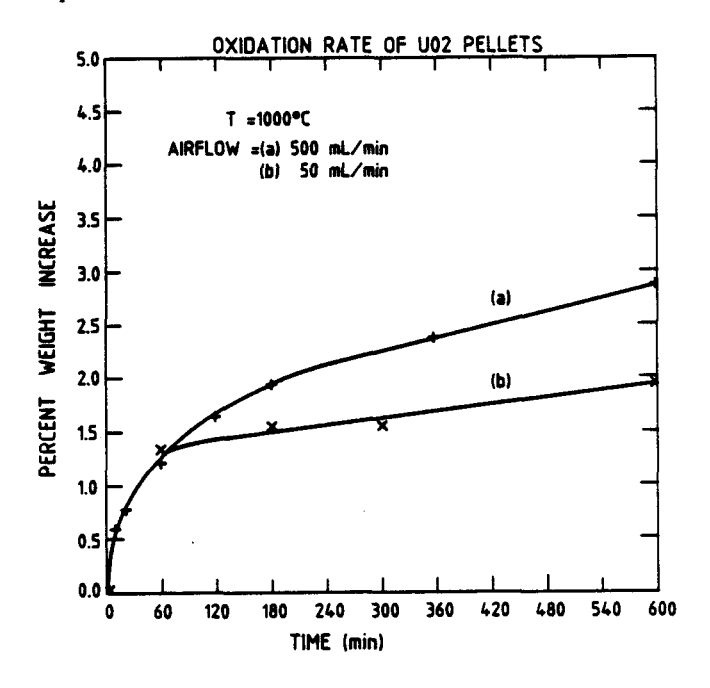


FIGURE 9: Oxidation at 1000°C.

Visually the appearance of pellets after oxidation was similar to that of pellets oxidized at $900\,^{\circ}\text{C}$ for much shorter times (Figure 10). The U_3O_8 surface layer is cracked and beneath this layer are other cracks many of which are radial penetrations into the pellet. At longer times, 10 hours, the pellet still retained its structure, but some large fragments, up to 8 mm in size, broke off during cutting for examination. The core was 100Z U₄O₉.

A transition phase of columnar grains was observed on the surface after 10 minutes oxidation. This is attributed to an intermediate between $\rm U_40_9$ and $\rm U_30_8$. At this short time, $\rm U_40_9$ was observed in the centre of pellets. At longer times, a tightly bonded layer of $\rm U_30_8$ surrounded the pellet and the structure of the pellet centre was equiaxed with only traces of Widmanstatten precipitation. Details of oxide thicknesses and X-ray analyses are given in Table 4.

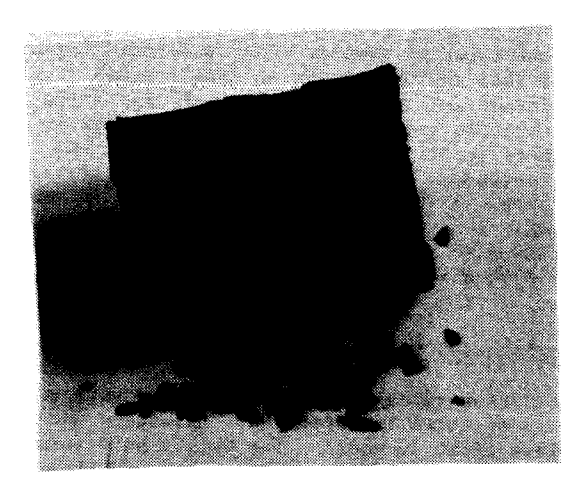


FIGURE 10: Pellet oxidized at 1000°C for 120 minutes with an airflow of 500 mL/min. The surface layer is U₃O₈. Beneath this layer, radial cracks partially penetrate the centre of the pellet. Magnification = 3X.

TABLE 4: OXIDATION PRODUCTS AT 1000°C

	500 cc/min		50 cc/min		
Time (min)	Interior	a ³ o ⁸	Interior	1308	
10	00_2 with 0_40_9 precip.	none			
60	70% U ₄ 0 ₉ 30% UO ₂	120 բա	-		
180	85% U ₄ O ₉ 15% UO ₂	450 կառ	85% U ₄ 0 ₉ 15% UO ₂	220 µm.	
600	100% U ₄ 0 ₉	900 µma	85% U ₄ 0 ₉ 15% UO ₂	700 µ na	

Results conclusively demonstrate that oxygen can diffuse much faster through $\rm UO_2/U_4O_9$ than through $\rm U_3O_8$ (see also reference 11).

Oxide Colours

 UO_2 powder is reddish brown; U_4O_9 is black; U_3O_7 is pink; U_3O_8 is black.

Oxygen Access

Although pellets lay on their sides, the line of contact between the pellet and crucible did not show reduced oxidation. There was no evidence of reduced cylindrical geometry implying that loose spalled $^{\rm U}_3{}^{\rm O}_8$ did not limit oxygen access.

Particle Size Analyses

Approximate particle size analysis is given in Table 5. Generally, the higher the oxidation rate,

the smaller is the particle size. Grain growth in the $\rm U_3^{0}8$ (larger crystals) is first seen at 700°C, rapidly increasing between 700 and 800°C.

COMPARISON WITH OTHER DATA

Bearing in mind structural differences in fuel from different sources, e.g. density, the above results are in excellent agreement with all other published data sets (1-3,6-10,17-22) except one (4,5) performed in static air, which probably suffered from air starvation.

TABLE 5: APPROXIMATE PARTICLE SIZE ANALYSIS

Temper- ature °C	Type of Material					
	Fragments		Particles		Powder	
	Size	wt%	Size	wt%	Size	wt%
400-600		0		0	10 µm	100
700	0.5 2022	20	100 կա	40	12 um	40
800	1.5 mm	50	330 µm.	25	12 µ m	25
900	3.5 mana	80	700 µma	10	16 µ առ	10
1000	6.0 mmz	90	700 µ ma	5	16 դ ո	5

RATE DETERMINING STEP

It is apparent from the above data, that oxygen diffusion through U308 is an important factor in governing the oxidation rate of ${\rm UO}_2$ in air. There are two distinct types of oxidation with a change in mechanism around 700°C. At temperatures ≤ 600°C, U_3O_8 spalls as small particles, 1-15 μm , as soon as it forms. At 700°C the U308 starts to form a cohesive structure in which grain growth occurs in the direction of the oxygen gradient. At higher temperatures $\geq 800\,^{\circ}\text{C}$ the U_3O_8 propagates by rapid grain growth, which sweeps through the grains of irradiated UO2, producing large crystals of U308, ≥1 mm. The larger the U308 crystals, the more difficult it is for oxygen to access the underlying ${\tt UO_2/U_4O_9}$ and the oxidation rate slows down. Oxidation is fastest at 500°C where the U308 offers little if any barrier to oxygen diffusion.

Generally it can be concluded that at all temperatures protective layers grown under conditions of slowly increasing oxygen partial pressure are more impermeable to oxygen than layers which are initially grown more rapidly at faster rising oxygen partial pressures. More ordered structures with fewer defects are grown at slower rates, and this is remembered by the protective layers long after the system is at atmospheric pressure.

Although no investigation of the effect of changing airflow is reported in the literature, the conclusions reported here are borne out by isobaric tests. Oxidation rates and diffusion coefficients were found to be pressure dependent in work at low temperatures (8), and high temperatures (6,8-10,23,24).

CO-EXISTENCE OF OXIDES

It is obvious from the data presented in this paper, that at any time during oxidation of a macroscopic sample at 400-1000°C when the weight gain is

between zero and 3.95%, i.e. intermediate between $\rm UO_2$ and $\rm U_3O_8$, several oxides are in co-existence, e.g. $\rm UO_2/U_4O_9/U_3O_7/U_3O_8$ at $\rm 400^{\circ}C$ and $\rm UO_2/U_4O_9/U_3O_8$ at $\rm 1000^{\circ}C$. At no time can a macroscopic sample in air consist of $\rm 100\%$ $\rm U_4O_9$ or $\rm 100\%$ $\rm U_3O_7$.

FISSION PRODUCT RELEASE STUDIES

Data most pertinent to understanding is presented. Zirconium furnace tubes and liners were used to oxidize fuel fragments in an environment chemically similar to that of a defected irradiated fuel element. It was subsequently discovered that the zirconium plays a most important part in reducing fission product releases.

Details of the apparatus are given in Figure 1.

Preliminary Experiments

These were the first experiments to demonstrate the reluctance of volatile fission products to come out of fuel under oxidizing conditions. Significant data is shown in Figure 11. In this experiment, 4.7 g of 0.3 MW.h/kg U fuel fragments were heated at 860°C with an airflow of 20 mL/min. Most of the volatile fission product release occurred during cooling while the fuel was at 400-600°C. The major fraction of the activity, 99%, was due to xenon. Early in the experiment small quantities of iodine were observed but no more iodine was seen deposited at the detector after the temperature of a steel pipe at the furnace outlet fell below 300°C. The volatile releases were very small, 0.05% of the xenon inventory and 0.004% of the iodine inventory. the furnace was pressurized to 50 psi and pressure was relieved downstream, the detectors immediately registered a large permanent rise in activity to 14500 cps above background. This was completely independent of flow rate. It is attributed to the dispersal of oxidized fuel dust. The spectrometer identified I-132, Np-239, Te-132 and other isotopes which had not been previously observed.

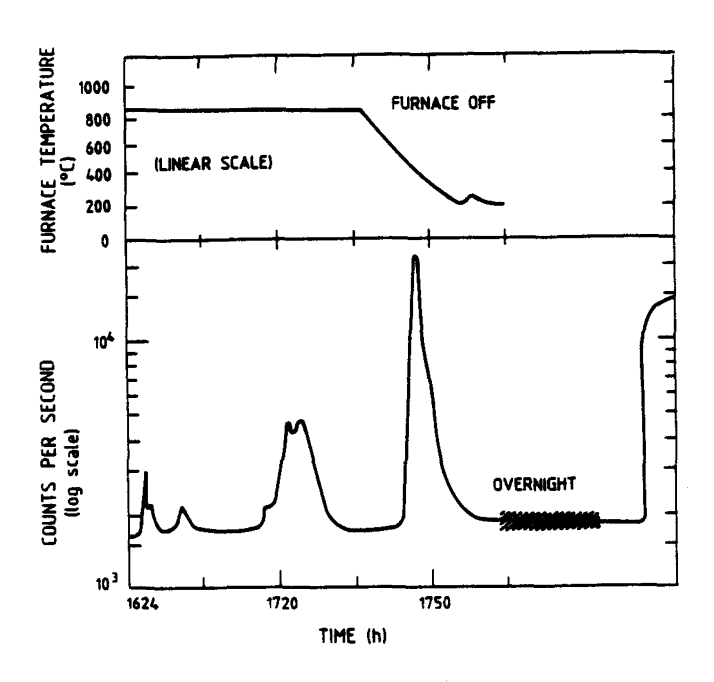


FIGURE 11: Activity release vs. time and temperature

Mostly the $\rm U_30_8$ was in the form of fine powder; ceramography of larger oxidized fuel fragments showed $\rm U_40_9$ overlying $\rm U0_2$, with only very small quantities of $\rm U_30_8$. This structure is very typical of that observed in unirradiated pellets oxidized at $400\text{--}500\,^{\circ}\text{C}$, which is the temperature range in which oxidation of $\rm U0_2$ is fastest. These results suggest that while at temperature, little oxidation of the $\rm U0_2$ occurred. The transient release observed on cooling is associated with an increased oxidation rate as the sample cooled from $600\text{--}400\,^{\circ}\text{C}$. At higher temperatures, the oxygen was presumably gettered by the zirconium components at the furnace. High temperature oxidation of the $\rm U0_2$ seems to have been almost negligible in this experiment.

Similar results were observed in two other experiments, the largest release being 1.4% of the xenon and 0.1% of the iodine for a sample given two oxidation treatments on successive days at 820°C and 910°C.

Significant Cs, Ru, and I deposition was noted in the vicinity of the furnace.

Low Burnup Fuel

Having been alerted by the previous experiments to the difficulty of oxidizing UO₂ at high temperatures in Zircaloy with small airflows, carefully controlled experiments were carried out using a smaller surface area of zirconium, and higher airflow introduced directly over the sample, which consisted of a 2 mm slice of Bruce pellet irradiated at 60 °C to 1.0 MW.h/kg U.

As in previous experiments, air was introduced to the sample after it had been brought to 920°C in argon (zero time in Figures 12 and 13).

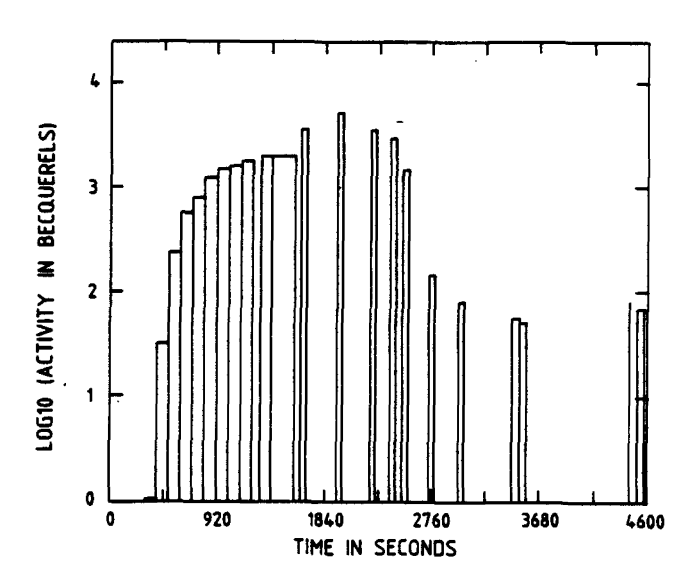


FIGURE 12: Kr-85m activity at 151.0 keV.

There was an immediate release of radioactive Xe and Kr isotopes. The volatile activity seen at the detector rose steadily until the furnace was switched off (1900 s) to stop the released activity becoming too high (>0.5 Mbq). After the furnace was switched

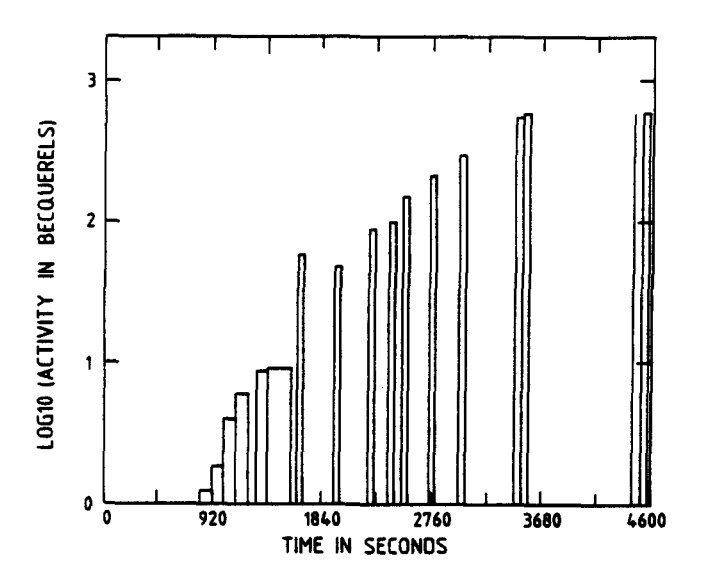


FIGURE 13: I-132 activity at 667.4 keV.

off, the activity due to noble gases immediately fell rapidly and in many cases this was an order of magnitude by the time the furnace was at 675°C (2700 s) (Figure 12). Fractional releases of noble gases varied from 15 to 26%.

The behaviour of iodine was totally different to that of the noble gases (Figure 13). In all cases the arrival of iodine isotopes at the detector was significantly later than the noble gases, causing the gross gamma activity to rise even after the furnace was shut off. The iodine activity at the on-line detector rose continually, only stabilizing after the furnace was isolated and bypassed. It appears that iodine moves slowly along the pipework as an adsorbed species. This was also observed in previous work. Whenever they were observed, the activities of I-131, 132, 133 and 135 were proportional to their calculated inventories implying identical chemical behaviour. The I-131 activity along the apparatus is shown in a logarithmic plot in Figure 14. The total release of I-131 was obtained by summing all the contributions from different parts of the apparatus. The result of 50% released iodine inventory is only approximate. Only 0.5% of the iodine reached the filters and traps, after flooding with a high flow of argon for 2-1/2 days before final shutdown. Most of the iodine was located in a small band 65 cm downstream of the furnace.

The distribution of Ru-103 was also highly localized, all of it being in the furnace. The total fractional release was identical to that of the iodine, 50%, and is subject to similar qualifications.

The total fractional release of Te-132 was only 6.6×10^{-3} of inventory. Less than 1% of this escaped from the furnace to the nearby outlet piping.

Gamma-ray spectrometry of some of the small oxidized fuel fragments, confirmed that substantial proportions of the Xe-133, I-131 and I-132 were retained in the fuel.

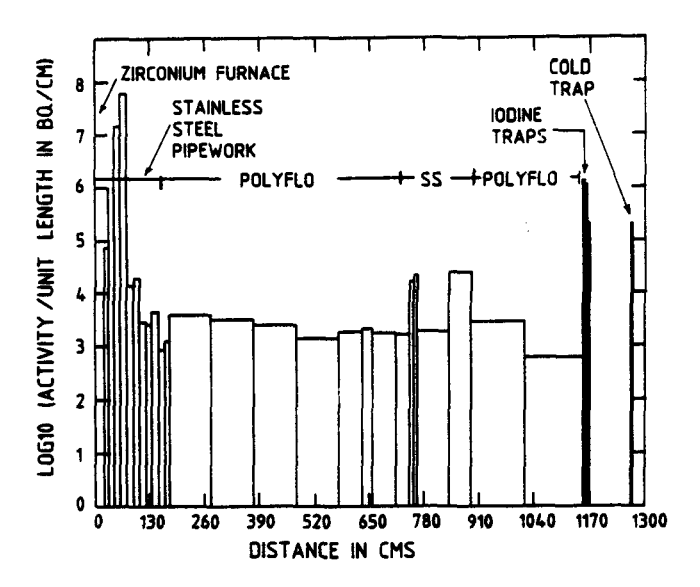


FIGURE 14: I-131 activity/cm along apparatus.

Ceramography of some of the oxidized fuel fragments showed that oxidation was incomplete $(\mathrm{UO}_2/\mathrm{U}_4\mathrm{O}_9)$ kernels were seen). Both the structure and the fragment size distribution were as expected from the unirradiated pellet data for oxidation at 920°C. According to the latter, approximately 30% of the sample should have been oxidized to $\mathrm{U}_3\mathrm{O}_8$. Allowing for the accuracy of the release measurements it seems that grain growth of $\mathrm{U}_3\mathrm{O}_8$ causes 100% release of Ru, I, Xe and Kr isotopes from the uranium oxide matrix.

Increasing releases measured by Parker et al. on raising the temperature from 800-1200°C (1) are probably due to increased oxidation of the samples rather than increased diffusional release.

High Burnup Fuel

In the first experiment, NRU experimental fuel of burnup 445 MW.h/kg U, was maintained at 950 \pm 20°C for 2.5 hours. In the second experiment, fuel of burnup 465 MW.h/kg U was maintained at temperature for 2 hours. In both cases the airflow was 100 mL/min and small fragments, \leq 3.0 mm, were used.

A repeat of the second experiment was used to record iodine and cesium deposition downstream of the furnace. This was not possible in the first two experiments which utilized some pipework in common, and which became heavily contaminated with both fission products and fuel dust after the first experiment.

Fragment sizes and ceramographic structures were as expected from the previous work on UO₂ oxidized at 900-1000°C.

Both fuels gave similar results. There was an immediate rise in activity as soon as the air reached the fuel (Figure 15). The Xe-133 activity peaked in about 11 minutes, and then decreased. An integrated release is shown in Figure 15a. Approximately 50% of the release occurs in 20 minutes and 100% in 60 minutes.

In the case of the second experiment, the measured release was identical to the calculated inventory.

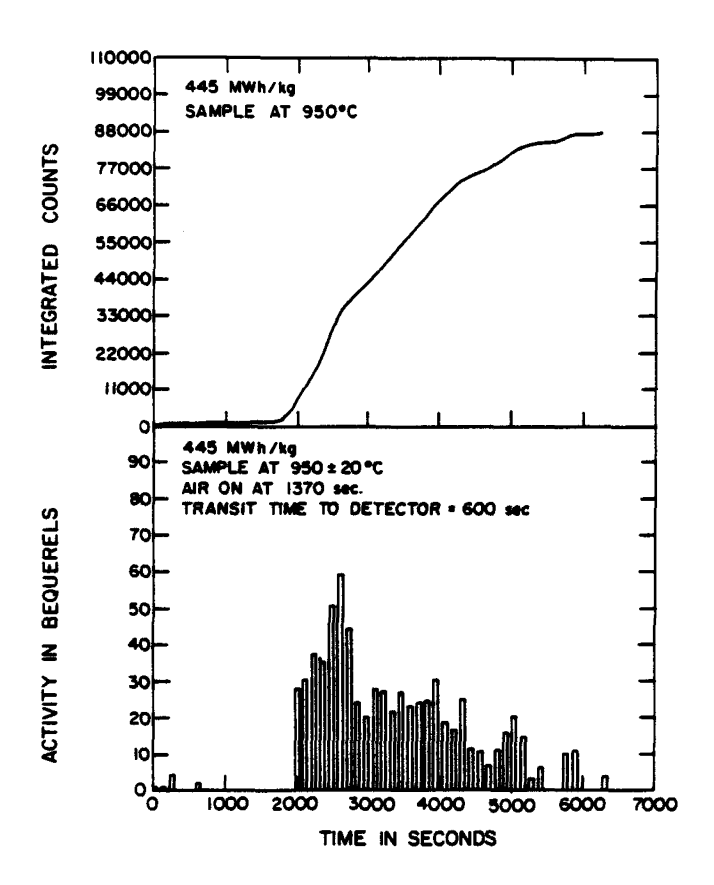


FIGURE 15: Xe-133 activity at 81.0 keV for 445 MW.h/kg fuel

- (a) integrated activity
- (b) on-line activity.

The measured release was larger than the calculated inventory for the first experiment possibly because this fuel was deliberately picked from the perimeter of an element whereas the other was picked from the interior of the element. Programs for calculating fission product inventories do not account for radial flux depression or increasing diffusional release at greater depths in the fuel pellets. It can safely be assumed that noble gas release was 100% in these experiments.

Iodine behaviour was as observed in previous experiments: a steady increase in activity at the detector location.

All components were connected with non-iodine absorbing polyethylene tubing except for two short sections of 20 cm length, each consisting of 6 mm bore stainless steel and carbon steel in parallel. After oxidizing fuel at 950°C for 2 hours, 20% of the pre-oxidation iodine inventory was located in the traps and 10% in the second steel section mostly on the carbon steel. The remaining 70% of the iodine was probably on the first steel section closer to the furnace but this could not be quantified because of cross contamination by fuel from other experiments. All results to date indicate that whatever its original form, iodine in fuel is oxidized to $\rm I_2$ when $\rm IO_2$ is oxidized to $\rm I_{30}$ at high temperatures.

In this experiment using predominantly polyethylene piping to minimize deposition of iodine en route to traps, at least 20% of the iodine inventory was sufficiently volatile to reach the traps 10 m from the furnace. Quantitatively the total iodine release from fuel during oxidation is probably similar to that of the noble gases, as observed previously.

Significant cesium release was also observed in these experiments, although the quantity, distribution and mass balance could not be obtained because of the contamination previously discussed, which is generally worse for cesium than for iodine. In experiment two, Cs-134, 136 and 137 were observed at the detector in quantities proportional to their fuel inventories, and at long times were in similar proportion to the I-131 also plated out on the pipework at the detector. The arrival time of cesium lagged behind the iodine by approximately 30 minutes. This is illustrated in Figure 16, where the ratio of cesium activity/iodine activity is plotted versus time. Although the cesium activity started off at a background level five times higher than the iodine, as soon as iodine release occurred, it fell behind; then slowly caught up until the oxidation transient at 4000 seconds caused a sudden increase in lodine concentration; the cesium then took another two thousand seconds to catch up. Activity observed prior to the oxidation, was due to movement of small quantities of Cs and I deposited during the first experiment. The final ratio of Cs-137 to I-131 was 1.15. The corresponding calculated ratio for the fuel inventories was 0.97. Since the iodine and cesium arrived at different times, it is obvious that they did not arrive as CsI, although the cesium may have subsequently reacted with adsorbed I2 to form CsI.

More recent experiments have confirmed that Cs and Ru are released 100% when $U0_2$ is oxidized to U_30_8 at $T \ge 850\,^{\circ}\text{C}$. Significant Sb release, 60%, was also observed.

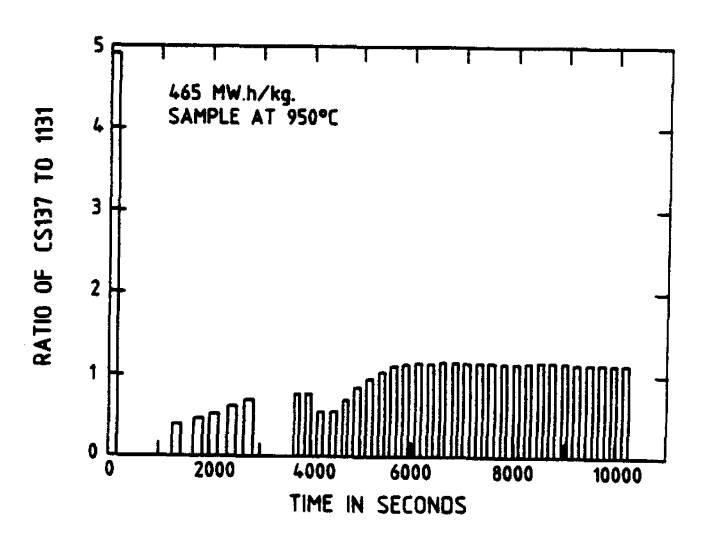


FIGURE 16: Ratio of Cs-137/I-131 activities for 465 MW.h/kg fuel.

Using the data on oxidation kinetics, the appropriate fragment size totally consumed in a given time under the conditions of this experiment can be

calculated. This is 20 minutes for a 0.6 mm fragment and 60 minutes for a 1.5 mm fragment.

These rate extrapolations from unirradiated fuel are in very good agreement with the present experiments on high burnup fuel if 100% release accompanies the formation of U_3O_8 by grain growth at these temperatures. Figure 15a can be thought of as showing the progression of oxidation of the fuel fragments to U_3O_8 , similar to Figure 9.

CONCLUSIONS

It has been observed that the grain growth of U_3O_8 at temperatures $\geq 800\,^{\circ}\mathrm{C}$ readily bridges small cracks and defects in the UO_2 (11,13). This should also be the case with defects induced by irradiation. Provided that the fragment size is correctly specified, it appears that oxidation rates are not significantly affected by burnup. The particle size and appearance of the product U_3O_8 are very similar to what is observed when unirradiated UO_2 is oxidized. It has been observed that many cracks intersect the boundary between the UO_2/U_4O_9 kernel and the U_3O_8 . These can allow fission gases to escape.

The greatest uncertainty in an accurate quantitative analysis is whether tunnels in high burnup fuel can increase oxygen availability at early times before they are closed by $\rm U_3O_8$ growth. In the present work this does not seem to have been significant.

Since releases of fission products are small below the temperature 700°C where grain growth in $\rm U_3O_8$ starts (1,9-11,22-26) and are 100% above the temperature 800°C where substantial grain growth occurs (1) then it may be postulated that grain boundary sweeping is responsible for the 100% releases rather than simple crystalline rearrangement from a cubic to an orthorhombic structure. Release rates correlate well with the movement of oxygen rather than diffusion of fission products. It is a corollary of the above argument that grain growth in $\rm UO_{2+x}$ will govern releases during oxidation in steam. In order to check this, further experiments are required including a study of noble gas diffusion in $\rm U_3O_8$.

The following isotopes are released 100% during oxidation of UO_2 to U_3O_8 at $T \ge 850\,^{\circ}\text{C}$: Xe, Kr, Cs, I, Sb and Ru. Tellurium release is also significant. All except the noble gases, rapidly plate out on metalwork.

 $\rm U_3 O_8$ dust is readily airborne and should be considered in accident analyses.

This work demonstrated the difficulty of oxidizing $\rm UO_2$ in the presence of Zr at high temperatures, confirmed later in experiments using whole elements (27). Whereas zirconium oxidation in air increases with temperature (28), the rate of oxidation of $\rm UO_2$ is fastest at $500\,^{\circ}{\rm C}$ and is very much slower at $1000\,^{\circ}{\rm C}$.

ACKNOWLEDGMENT

Special thanks are due to R.D. Barrand, N.M. Melcher and L.F. Woo for their technical assistance,

and to C. Blahnik for his interest and encouragement.

Part of the work described here was funded by CANDEV, a cooperative development program between Atomic Energy of Canada Limited and Ontario Hydro.

REFERENCES

- (1) PARKER, G.W. et al., "Out-of-Pile Studies of Fission-Product Release from Overheated Reactor Fuels at ORNL, 1955-1965", ORNL-3981, UC-80, 1967.
- (2) PEAKAL, K.A. and ANTILL, J.E., "Oxidation of Uranium Dioxide in Air at 350-1000°C", J. Nucl. Mat., 2, 194 (1960).
- (3) BOASE, D.G. and VANDERGRAAF, T.T., "The Canadian Spent Fuel Storage Canister: Some Materials Aspects", Nucl. Tech., 32, 60 (1977).
- (4) IWASAKI, M. and ISHIKAWA, N., "Air-Oxidation of UO₂ Pellets at 800 and 900°C, J. Nucl. Mat., 36, 116 (1970).
- (5) IWASAKI, M., SAKURAI, T., ISHIKAWA, N. and KOBAYASHI, Y., "Oxidation of UO₂ Pellets in Air", J. Nucl. Sci. and Tech., 5, 652 (1968).
- (6) DHARWADKAR, S.R. and KARKHANAVALA, M.D., "High Temperature Oxidation of Uranium Dioxide: Part II - Pressure and Temperature Dependence of the Oxidation Rate", Indian J. Chem., 10, 1179 (1972); IBID, 13, 685 (1975).
- (7) FURUICHI, R., ISHII, T. and NAKANE, T., "Thermoanalytical Study on the Oxidation of Uranium Dioxides Derived from Uranyl Nitrate, Uranyl Acetate and Ammonium Diuranate", Thermochimica Acta, 33, 51 (1979).
- (8) ANDERSON, J.S., ROBERTS, L.E.J. and HARPER, E.A., "The Oxides of Uranium, Part VII, The Oxidation of Uranium Dioxide", J. Chem. Soc., p. 3946 (1955).
- (9) PETERSON, S.F., CADIEUX, J.R. et al., "Chemical Studies for Alternate Fuel Cycles at the Savannah River Laboratory", DP-MW-80-38, 1980.
- (10) STONE, J.A., "Voloxidation Studies with UO₂ Reactor Fuels", in Fuel Cycles for the 80's, CONF-800943, 1980.
- (11) MCCRACKEN, D.R., "Oxidation of UO₂ at 400-1000°C in Air and its Relevance to Fission Product Release", Atomic Energy of Canada Limited Report, AECL-8642, in preparation for publication.
- (12) MCCRACKEN, D.R., WOO, L.F. and MELCHER, N.M., "Visual and Metallographic Appearance of UO₂ Pellets Oxidized in Air at 400-600°C", unpublished report no. CRNL-2790, 1984, Atomic Energy of Canada Limited Report, Research Company, Chalk River, Ontario, KOJ 1JO.

- (13) MCCRACKEN, D.R., WOO, L.F. and MELCHER, N.M., "Visual and Metallographic Investigation of UO₂ Pellets Oxidized in Air at 700-1000°C", unpublished report no. CRNL-2829, 1985, Atomic Energy of Canada Limited Report, Research Company, Chalk River, Ontario, KOJ 1JO.
- (14) Data cards issued annually by Joint Committee on Powder Diffraction Standards, International Centre for Diffraction Data, 1601 Park Lane, Swarthmore, Pa. 19081.
- (15) TUXWORTH, R.H. and EVANS, W., "Habit Planes for U₄O₉ Precipitation in Uranium Dioxide", J. Nucl. Mat., 1, 302 (1959).
- (16) SCHANER, B.E., "Metallographic Determination of the UO₂-U₄O₉ Phase Diagram", J. Nucl. Mat., 2, 110 (1960).
- (17) HASTINGS, I.J., MCCRACKEN, D.R., NOVAK, J. and NASH, K., "Behaviour in Air at 175-400°C of Irradiated UO₂ Fuel", invited presentation at the International Workshop on "Irradiated Fuel Storage Operating Experience and Development Programs", Toronto, Ontario, 1984 October 17-18, Atomic Energy of Canada Limited Report, AECL-8562.
- (18) TAYLOR, P., BURGESS, E.A. and OWEN, D.G., "An X-Ray Diffraction Study of the Formation of Beta-UO_{2.33} on UO₂ Pellet Surfaces in Air at 229 to 275°C", J. Nucl. Mat., 88, 153 (1980).
- (19) SIMPSON, K.A. and WOOD, P., "Uranium Dioxide Fuel Oxidation in Air Below 350°C", Proc. NRC. Workshop, "Spent Fuel/Cladding Reaction During Dry Storage", NUREG/CP-0049, p. 70 plus Appendix D-1, Gaithersburg, MD., 1983 August 17-18.
- (20) WHITE, G.D. and GILBERT, E.R., "UO₂ Oxidation at Low Temperatures in Air", PNL-SA-11711, CONF-8310175-2, 1983.
- (21) ARONSON, S., ROOF, R.B., Jr., and BELLE, J., "Kinetic Study of the Oxidation of Uranium Dioxide", J. Chem. Phys., 27, 137 (1957).
- (22) TENNERY, V.J., "The Oxidation of UO₂ and (U,Pu)O₂ - A Thermogravimetric and X-Ray Diffraction Study", p. 23, in "Voloxidation -Removal of Volatile Fission Products from Spent LMFBR Fuels", R.D. Baybarz et al., edited by J.H. Goode, ORNL-TM-3723, UC-796, 1973.
- (23) CADIEUX, J.R. and STONE, J.A., "Voloxidation and Dissolution of Irradiated Plutonium Recycle Fuels", DP-MS-80-10, 1980.
- (24) WATSON, C.D. and CLINTON, S.D., "Engineering Data", p. 126, "Voloxidation - Removal of Volatile Fission Products from Spent LMFBR Fuels", R.D. Baybarz et al., edited by J.H. Goode, ORNL-TM-3723, UC-796, 1973.
- (25) GOODE, J.H. and VAUGHEN, V.C.A., "Voloxidation Tests with Irradiated Fuels", p. 119, "Voloxidation - Removal of Volatile Fission Products from Spent LMFBR Fuels", R.D. Baybarz et al., edited by J.H. Goode, ORNL-TM-3723, UC-796, 1973.

- (26) STONE, J.A. and JOHNSON, D.R., "Measurement of Radioactive Gaseous Effluents from Voloxidation and Dissolution of Spent Nuclear Fuel", 15th DOE Nuclear Air Cleaning Conference, p. 570-583, CONF-780819, 1978.
- (27) HASTINGS, I.J., MCCRACKEN, D.R., BARRAND, R.D., KELM, J.R. and NOVAK, J., "Post-Irradiation Dimensional Stabilities and Fission Product Behaviour of Defected UO₂ Fuel at 400, 600 and 900°C in Air", presented at ACS Annual Meeting, Cincinatti, 1985 May 5-9, to be published in Advances in Ceramics.
- (28) PROBST, M.B., EVANS, E.B. and BALDWIN, W.M., Jr., "Scaling of Zirconium at Elevated Temperatures", AECU-4113, 1959.